

Critical behavior and universality in Lévy spin glasses

Juan Carlos Andresen,¹ Katharina Janzen,² and Helmut G. Katzgraber^{3,1}

¹*Theoretische Physik, ETH Zurich, CH-8093 Zurich, Switzerland*

²*Institut für Physik, Carl-von-Ossietzky-Universität, 26111 Oldenburg, Germany*

³*Department of Physics and Astronomy, Texas A&M University, College Station, Texas 77843-4242, USA*

(Dated: May 17, 2011)

Using large-scale Monte Carlo simulations that combine parallel tempering with specialized cluster updates, we show that Ising spin glasses with Lévy-distributed interactions share the same universality class as Ising spin glasses with Gaussian or bimodal-distributed interactions. Corrections to scaling are large for Lévy spin glasses. In order to overcome these and show that the critical exponents agree with the bimodal and Gaussian case, we perform an extended scaling of the two-point finite size correlation length and the spin-glass susceptibility. Furthermore, we compute the critical temperature and compare its dependence on the disorder distribution width to recent analytical predictions [J. Stat. Mech. (2008) P04006].

PACS numbers: 75.50.Lk, 75.40.Mg, 05.50.+q

I. INTRODUCTION

Although universality has been established for many systems without disorder and frustration, there are still skeptics that question this cornerstone of the theory of statistical mechanics when applied to disordered spin systems with frustrated interactions. According to universality, the values of quantities such as critical exponents, do not depend on microscopic details of the model, but only on e.g., the space dimension and the symmetry of the order parameter. Arguments based on high-temperature series expansions¹ support universality and there is no a priori reason why systems with both disorder and frustration, such as spin glasses,² might not show universal features. However, numerical studies are difficult^{3–28} and suffer from strong corrections to scaling. Therefore, there is still debate^{11,16,18,21,29} for some model systems if the shape of the disorder distribution can influence the universality class of the system.

Although it is now well established that universality is not violated for nearest-neighbor spin glasses with compact disorder distributions (e.g., Gaussian or bimodal),^{22,26,27} some studies suggest that this might not be the case when the disorder distributions are broad.¹⁸ If the spin interactions are drawn from a Gaussian or bimodal distribution the probability to have extremely large interactions is very small. It is, however, unclear if strong couplings between the spins change the universality class of the system. Selecting the interactions between the spins from a Lévy distribution allows one to continuously tune the probability to have very strong bonds in the system. In particular, for $\alpha < 2$ (see below for details) the Lévy distribution has broad tails and thus the probability to have a strong bond between two spins is large, especially in the limit $\alpha \rightarrow 1$.

Using large-scale Monte Carlo simulations that combine parallel tempering with specialized cluster moves,³⁰ as well as extended scaling techniques,²⁴ our results show that Lévy spin glasses do obey universality for the system sizes studied. Our estimates of the critical ex-

ponents agree within error bars with the best known estimates^{26,27} for Gaussian and bimodal disorder. Furthermore, we probe recent analytical predictions³⁰ made for the critical temperature of Lévy spin glasses as a function of the disorder distribution width.

The paper is structured as follows: In Sec. II we introduce the model studied, as well as the measured observables. Section III outlines the special (cluster) algorithm used to treat strong interactions in the Lévy spin glass, the finite-size scaling analysis, and how we estimate the critical temperature, followed by results presented in Sec. IV, as well as concluding remarks.

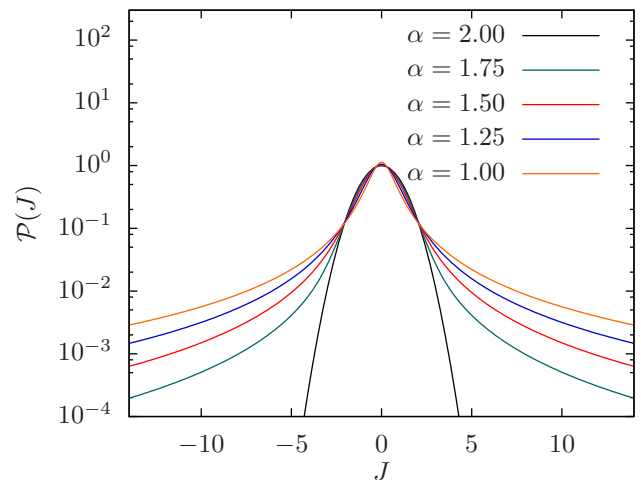


FIG. 1: (Color online) Lévy distribution $\mathcal{P}(J)$ for the different values of the shape parameter α and $c = 1/\sqrt{2}$, as studied here. In particular, for $\alpha = 2$ a Gaussian distribution is recovered. For $1 \leq \alpha < 2$ the distribution is fat-tailed, as can be seen in the linear-log plot.

II. MODEL AND OBSERVABLES

We study the critical behavior of the Edwards-Anderson Ising spin glass³¹ with Lévy-distributed interactions, i.e.,

$$\mathcal{H} = - \sum_{\langle i,j \rangle} J_{ij} S_i S_j, \quad (1)$$

where the sites i lie on a three-dimensional cubic lattice of size $N = L^3$, L the linear dimension, and the spins S_i can take the values ± 1 . Periodic boundary conditions are used to reduce corrections to scaling. The sum is over nearest neighbors and the interactions J_{ij} are independent random variables taken from a Lévy distribution with zero mean and $c = 1/\sqrt{2}$ defined through the characteristic function $\phi(t)$ as

$$\mathcal{P}(J) = \frac{1}{2\pi} \int_{-\infty}^{+\infty} dt \phi(t) e^{-itJ} = \frac{1}{2\pi} \int_{-\infty}^{+\infty} dt e^{-itJ - |ct|^\alpha}. \quad (2)$$

The parameter α influences the shape of the distribution and, in particular, the width of the tails. For $\alpha = 2$ Eq. (2) reduces to a Gaussian with variance $\sigma = \sqrt{2}c$. When $1 \leq \alpha < 2$ the tail of the distribution decays as a power law, as seen in Fig. 1. In this case, exchange interactions with very large values can occur, albeit with small probability. However, such strong interactions form “dimers” of spins that cannot be flipped with standard Monte Carlo methods.³² For decreasing α the probability to have dimers grows, as well as the average of the maximum exchange interaction value.

To test universality, at least two independent critical exponents need to be computed. Therefore, in the simulations, we measure the following quantities.

The spin overlap q is defined as

$$q = \frac{1}{N} \sum_i S_i^{(1)} S_i^{(2)}, \quad (3)$$

where (1) and (2) are two copies of the system with identical disorder. Using q we define the Binder ratio³³ g via

$$g = \frac{1}{2} \left(3 - \frac{[\langle q^4 \rangle]_{\text{av}}}{[\langle q^2 \rangle]_{\text{av}}^2} \right) \sim \tilde{G}[L^{1/\nu}(T - T_c)], \quad (4)$$

where $\langle \dots \rangle$ represents a thermal average and $[\dots]_{\text{av}}$ an average over the disorder. The Binder ratio is a dimensionless function \tilde{G} , i.e., data for different system sizes cross at a putative transition temperature T_c . A finite-size scaling analysis of the universal function³⁴ \tilde{G} allows one to determine the critical exponent ν for the correlation length.

The spin-glass susceptibility χ_{SG} is defined as

$$\chi_{\text{SG}} = N [\langle q^2 \rangle]_{\text{av}} \sim L^{2-\eta} \tilde{C}[L^{1/\nu}(T - T_c)]. \quad (5)$$

A finite-size scaling analysis of the susceptibility thus permits the calculation of the critical exponent η . However,

a simple scaling analysis of the spin-glass susceptibility suffers from strong corrections to scaling²⁶ and therefore an extended scaling²⁴ is performed below where the scaling function incorporates corrections derived from the resummation of a high-temperature series expansion.

Finally, we measure the two-point finite-size correlation length.^{15,17} To do so we introduce the wave-vector-dependent spin-glass susceptibility

$$\chi_{\text{SG}}(\mathbf{k}) = \frac{1}{N} \sum_{i,j} [\langle S_i S_j \rangle]_{\text{av}} e^{i\mathbf{k}(\mathbf{R}_i - \mathbf{R}_j)}. \quad (6)$$

The two-point finite-size correlation length ξ_L is then given by

$$\xi_L = \frac{1}{2 \sin(k_{\text{min}}/2)} \sqrt{\frac{\chi_{\text{SG}}(\mathbf{0})}{\chi_{\text{SG}}(\mathbf{k}_{\text{min}})} - 1}, \quad (7)$$

where $\mathbf{k}_{\text{min}} = (2\pi/L, 0, 0)$. It scales as

$$\frac{\xi_L}{L} = \tilde{X}[L^{1/\nu}(T - T_c)], \quad (8)$$

i.e., whenever $T = T_c$ data for different system sizes cross at one point, up to corrections to scaling.²⁷

III. NUMERICAL DETAILS

To test for universal behavior a detailed numerical study needs to be performed where one has to ensure that the data are in thermal equilibrium. For this purpose we use a special cluster algorithm that ensures that spin dimers flip in reasonable simulation times. In addition, we describe the data analysis used.

A. Algorithm

The simulations are done using the parallel tempering Monte Carlo method³⁵ combined with a special cluster flip algorithm³⁰ that ensures ergodic behavior even in the presence of excessively strong exchange interactions between few spins.

Because the Lévy distribution has power-law decaying tails, for certain values of the parameter α the exchange interactions J_{ij} can be very large. If two spins have a strong interaction they will be virtually “frozen” under single-spin-flip dynamics. To avoid extremely long equilibration times, at the beginning of each simulation different sets of clusters C_n are generated.³⁰ The generation of the sets C_n is done the following way:

1. Set $J_{\text{min}}^0 = T_{\text{max}}/4$, where T_{max} is the maximal temperature from the simulated temperature set.
2. The clusters in set C_n consist of spins connected by bonds that satisfy $|J_{ij}| > J_{\text{min}}^n$.

3. The cluster set C_n is stored if $C_n \neq C_{n-1}$ (or if $n = 0$).
4. J_{\min}^n is iteratively incremented by one ($J_{\min}^{n+1} = J_{\min}^n + 1$). The procedure is repeated initiating from step two until C_n consists only of clusters of size 2. During the procedure all clusters are stored.

One Monte Carlo sweep consists of the following procedure: Each spin of the system is picked once. After having picked the spin, a single-spin flip is performed with probability $p = 0.75$ (empirically we find that for $p \sim 0.75$ equilibration is fastest), otherwise a cluster move is done. In particular:

- *The single spin flip* is done with the Metropolis probability $\min\{1, \exp(-\Delta E/T)\}$, where ΔE is the energy difference between the current configuration and the configuration with the spin flipped.
- *The cluster flip* algorithm works as follows: One cluster from all sets is randomly (uniformly) picked and flipped with the Metropolis probability $\min\{1, \exp(-\Delta E/T)\}$, where ΔE is the difference between the energy of the actual configuration and the configuration with the cluster flipped. The cluster flip is independent of the orientation of the spins in the cluster, i.e., the clusters contain only spin indices, such that each spin in the cluster can change the direction by other update steps.

Note that typical cluster sizes range from 2–20 spins.

Because the equilibration test for Gaussian disorder³⁶ does not work when the disorder is Lévy distributed, the equilibration is monitored by logarithmic binning. All measured observables (and their higher moments) are recorded as a function of simulation time. Once the last four bins agree within error bars the system is deemed to be in thermal equilibrium. If this test is not passed, the simulation time is increased by a factor of 2 until this is the case. Simulation parameters are summarized in Table I.

B. Finite-size scaling analysis

To gain insights on the strength of the corrections to scaling, we can compare two dimensionless quantities,^{22,26} the correlation length ξ_L/L and the Binder parameter g . By plotting $g[\xi_L(T, L)/L]$ there are no nonuniversal metric factors. Therefore, data for all system sizes simulated and a given parameter α should all collapse onto a universal function if there are no corrections to scaling. Data for $\alpha = 1.25$ are shown in Figure 2 and illustrate that corrections are large for $L \lesssim 8$.

Furthermore, if two different models share the same critical exponent ν , because no nonuniversal factors when plotting $g[\xi_L(T, L)/L]$ are present, all data should collapse onto a universal curve. In Fig. 2 we also show data for Gaussian disorder ($\alpha = 2$) for a large system size

TABLE I: Parameters of the simulations for different α values. N_{sa} is the number of samples, N_{sw} is the total number of Monte Carlo sweeps used for equilibration (the same amount is used for measurement), T_{\min} is the lowest temperature simulated, T_{\max} is the highest temperature simulated, and N_T is the number of temperatures used in the parallel tempering method for each system size L .

α	L	N_{sa}	N_{sw}	T_{\min}	T_{\max}	N_T
1.00	4	6000	65536	1.112	2.000	12
1.00	6	4830	252144	1.112	2.000	12
1.00	8	3737	1048576	1.112	2.000	12
1.00	10	3400	4194304	1.112	2.000	12
1.00	12	3995	16777216	1.112	2.000	12
1.00	14	1118	33554432	1.305	1.896	8
1.25	4	5600	65536	0.898	1.704	13
1.25	6	5082	262144	0.898	1.704	13
1.25	8	4165	1048576	0.898	1.704	13
1.25	10	4995	2097152	0.898	1.704	13
1.25	12	2998	16777216	0.898	1.704	13
1.50	4	5040	65536	0.726	1.452	14
1.50	6	4958	262144	0.726	1.452	14
1.50	8	5083	1048576	0.726	1.452	14
1.50	10	3014	2097152	0.726	1.452	14
1.50	12	3006	16777216	0.726	1.452	14
1.75	4	5040	65536	0.618	1.305	15
1.75	6	5016	262144	0.618	1.305	15
1.75	8	4592	1048576	0.618	1.305	15
1.75	10	4794	2097152	0.618	1.305	15
1.75	12	3999	16777216	0.618	1.305	15

($L = 24$).²⁶ Data for $\alpha = 1.25$ and $L \gtrsim 8$ agree with the Gaussian case, thus illustrating that for a conventional scaling analysis only the largest system sizes should be included.

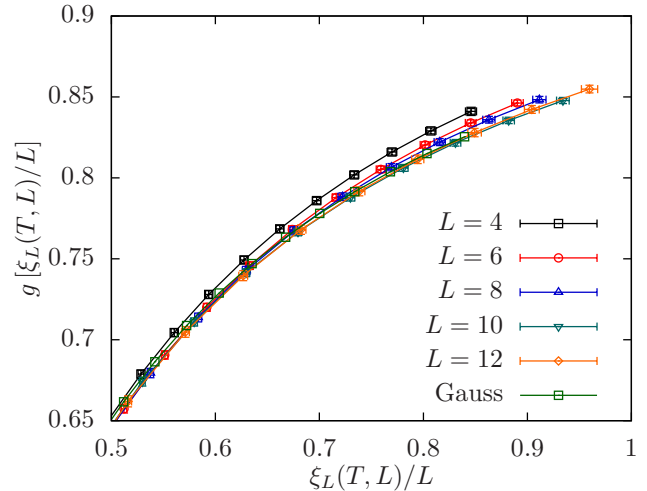


FIG. 2: (Color online) Binder ratio g as a function of the finite-size correlation length ξ_L/L for several system sizes and for a Lévy parameter $\alpha = 1.25$. Strong corrections to scaling are visible. The data for the largest system sizes simulated agree with the Gaussian case ($\alpha = 2$, $L = 24$, from Ref. 26).

We have attempted different scaling approaches,^{22,26} as well as the inclusion of corrections to scaling.²⁷ How-

ever, large system sizes are difficult to simulate for Lévy spin glasses and therefore we use the extended scaling technique²⁴ that allows us to include smaller system sizes in the scaling analysis.

Within the extended scaling framework²⁴ the standard scaling expression for the correlation length, Eq. (8), is replaced by

$$\frac{\xi_L}{L} \sim \tilde{X}[(LT)^{1/\nu}|1 - (T/T_c)^2|]. \quad (9)$$

The aforementioned expression is derived by including a resummation of a high-temperature series expansion and therefore includes effects of corrections to scaling. Similarly, the scaling relation for the susceptibility, Eq. (5), is replaced by

$$\chi_{SG}(L, T) \sim (LT)^{2-\eta} \tilde{C}[(LT)^{1/\nu}|1 - (T/T_c)^2|]. \quad (10)$$

We assume that the scaling function in Eq. (9) can be approximated by a third-order polynomial for temperatures larger than T_c , i.e., $\tilde{X}(x) = a + bx + cx^2 + dx^3$ where $x = (LT)^{1/\nu}|1 - (T/T_c)^2|$, $T > T_c$ and perform a fit to the six parameters a, b, c, d, T_c and ν . A similar approach is used for the spin-glass susceptibility [Eq. (10)], for which there is a seventh parameter, the critical exponent η . Note that the extended scaling scheme only works for temperatures $T > T_c$. Therefore, we first perform a rough estimate of T_c using conventional scaling methods. The nonlinear fit is performed with the statistics package R,³⁷ including system sizes $L \geq 6$. Error bars are determined using a bootstrap analysis.

To compute the error bars we apply the following procedure: For each system size L and N_{sa} disorder realizations, a randomly selected bootstrap sample of N_{sa} disorder realizations is generated. With this random sample, an estimate of the different observables is computed for each temperature. We repeat this procedure $N_{boot} = 500$ times for each lattice size and then assemble N_{boot} complete data sets (each having results for every size) by combining the i -th bootstrap sample for each size for $i = 1, \dots, N_{boot}$. The finite-size scaling fit described above is then carried out on each of these N_{boot} sets, thus obtaining N_{boot} estimates of the fit parameters. Because the bootstrap sampling is done with respect to the disorder realizations which are statistically independent, we can use a conventional bootstrap analysis to estimate statistical error bars on the fit parameters. These are comparable to the standard deviation among the N_{boot} bootstrap estimates.²⁶

From the aforementioned finite-size scaling we can also extract the critical temperature $T_c(\alpha)$ to compare to analytical predictions. We use the critical temperature estimated using the extended scaling method for the correlation length [Eq. (9)] because corrections to scaling are smaller than for the spin-glass susceptibility. Furthermore, the bootstrap analysis requires one parameter less leading to smaller statistical errors.

TABLE II: Summary of estimates of the critical parameters. T_c^ξ and ν^ξ are the critical parameters estimated from an extended scaling analysis of the two-point correlation length, whereas η^χ has been computed from a finite-size scaling analysis of the spin-glass susceptibility with T_c, ν and η as free parameters. $\eta^\chi|_{T_c, \nu}$ is computed from a finite-size scaling analysis of the susceptibility with $T_c = T_c^\xi$ and $\nu = \nu^\xi$ fixed and only η as a parameter.

α	T_c^ξ	ν^ξ	η^χ	$\eta^\chi _{T_c, \nu}$
1.00	1.467(31)	2.42(17)	-0.346(220)	-0.438(26)
1.25	1.209(28)	2.49(17)	-0.411(209)	-0.412(20)
1.50	1.094(21)	2.34(15)	-0.344(274)	-0.414(20)
1.75	0.996(20)	2.61(19)	-0.274(224)	-0.413(17)

IV. RESULTS

Corrections to scaling for small systems of Lévy spin glasses with $1 \leq \alpha < 2$ are large (see Fig. 2). We attempt to scale the data using the extended scaling scheme, as shown in Fig. 3 (center and right columns). The left column shows the finite-size correlation length for different values of the parameter α . In all cases the data cross at a transition temperature that decreases with increasing α . In the center panels of Fig. 3 we show an extended scaling of the two-point finite size correlation length according to Eq. (9) with the critical exponents ν and T_c as parameters. The right column of Fig. 3 shows an extended scaling of the spin-glass susceptibility according to Eq. (10) with η, ν and T_c as free parameters. The scaling of the data works well and, in particular, the estimated critical exponents agree with the bimodal values.²⁷ Our best estimates are summarized in Table II. Furthermore, in Fig. 4 we compare our estimates for η and ν to the bimodal estimates [$\eta = -0.375(10)$ and $\nu = 2.45(15)$].²⁷ The data therefore suggest that all studied Lévy spin glasses share the same universality class.

To further strengthen our results for the finite-size correlation length, in Fig. 5 we show $g[\xi_L(L, T)/L]$ for the largest system size studied and different α , as well as data for Gaussian disorder.²⁶ The data collapse cleanly onto a universal curve without any scaling parameters providing further evidence for universal behavior. The inset of Fig. 5 shows $\xi_L/L(T = T_c)$ for different values of the exponent α . For all cases the data agree within error bars with the best estimate for bimodal disorder²⁷ hence strengthening our claim for universal behavior.

Finally, we show in Fig. 6 estimates for the critical temperature T_c as a function of the exponent α .^{30,38} The horizontal blue line represents the Gaussian limit.^{26,27} The red curve represents $T_c(\alpha)$ for a mean-field spin-glass model on a diluted graph with fixed connectivity $k + 1 = 6$. The critical temperature is determined from the following equation

$$1 = k \int dJ \mathcal{P}(J) \tanh^2(J/T_c), \quad (11)$$

where $\mathcal{P}(J)$ is given by Eq. (2).³⁹ There is qualitative

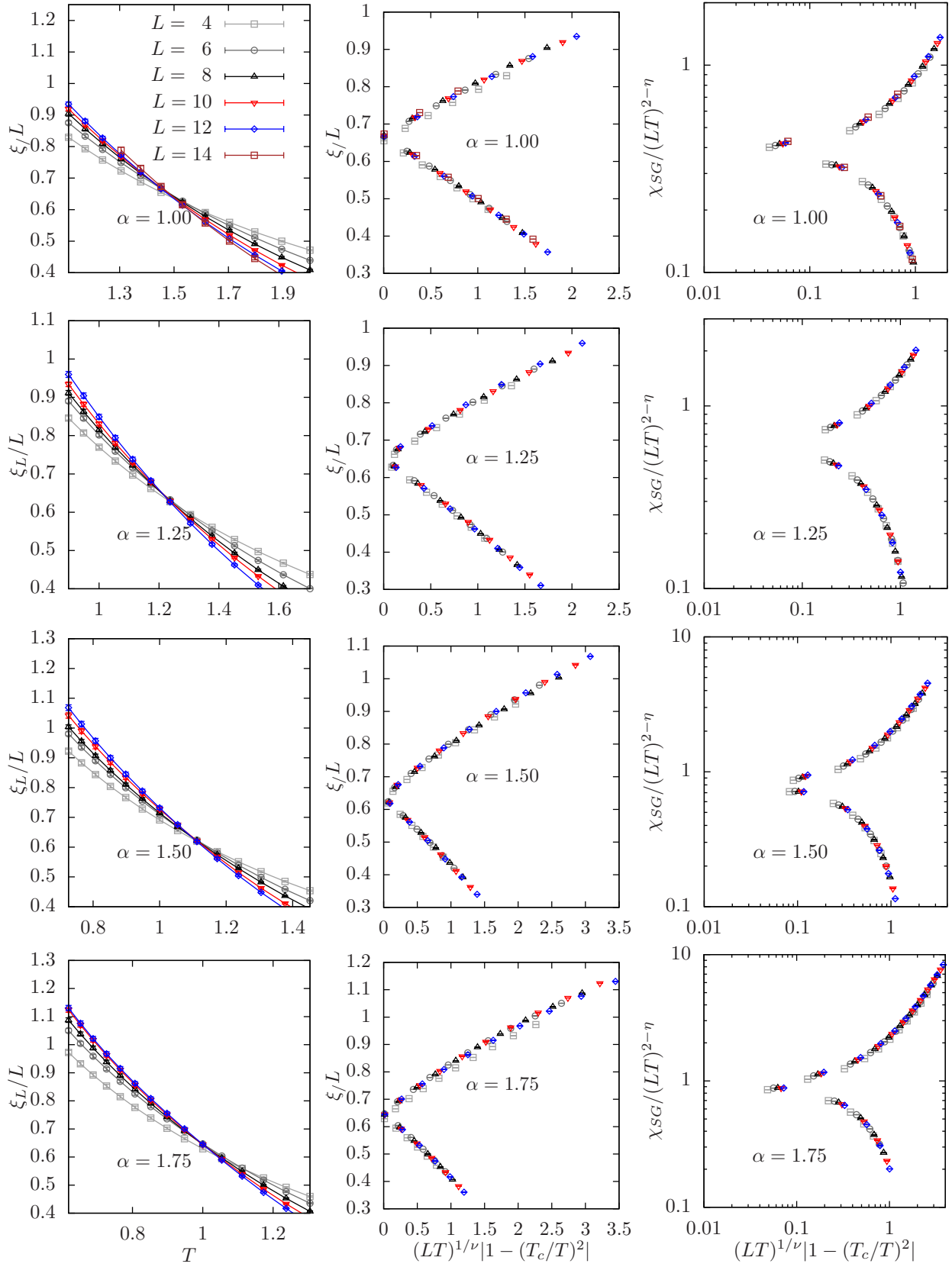


FIG. 3: (Color online) Left: Two-point finite-size correlation length ξ_L/L as a function of the temperature T for different Lévy parameters α . The data cross, thus signaling the presence of a transition. Center: Extended scaling of the two-point finite-size correlation length for different α . Right: Extended scaling of the spin-glass susceptibility for different α . The data scale very well and the critical exponents extracted from the scaling agree within error bars, thus suggesting that all systems share the same universality class. See Table II for the optimal scaling parameters.

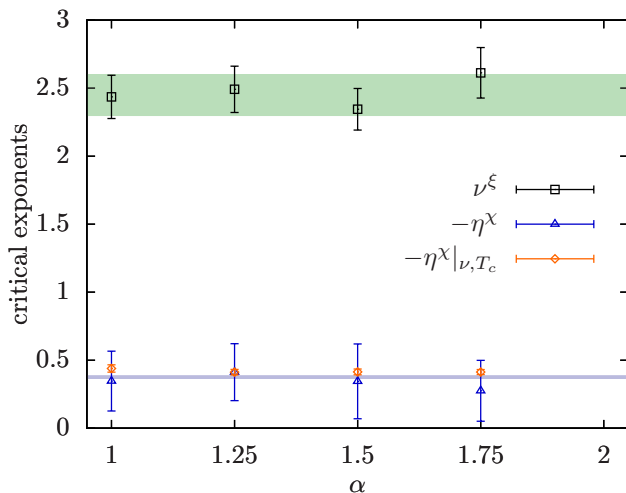


FIG. 4: (Color online) Critical exponents η and ν as a function of the Lévy parameter α . The shaded areas correspond to the estimates for Bimodal disorder from Ref. 27. The estimate for the critical exponent ν^ξ comes from an extended finite-size scaling analysis of the two-point correlation length. The estimates for the critical exponent η are from two independent analyses of the spin-glass susceptibility. η^ξ is computed from an extended finite-size scaling analysis where η , ν , and T_c are parameters, whereas $\eta^\xi|_{\nu,T_c}$ is computed by fixing $\nu = \nu^\xi$ and $T_c = T_c^\xi$ from the analysis of the two-point correlation length. For all values of α studied, the exponents ν^ξ and η^ξ are in good agreement with the best-known estimates for the bimodal case. However, the estimate for $\eta^\xi|_{\nu,T_c}$ consistently lies above the best estimate for η possibly due to strong corrections to scaling that we cannot account for, as well as systematic errors from the determination of ν^ξ .²⁶

agreement in the trend of the data. At first sight, there is a disagreement to the behavior obtained for the infinite-range model studied in Refs. 40 and 30, because the dependence on α is reversed in that case. However, the large connectivity limit of Eq. (11) amounts to the expression for the critical temperature stated in Refs. 40 and 30. For the infinite-range model an α -dependent rescaling of the couplings ($J_{ij} \rightarrow J_{ij}N^{-1/\alpha}$) is necessary to obtain a non-trivial thermodynamic limit which changes the energy scale in an α -dependent way.

V. CONCLUSIONS

We have studied the critical behavior of a three-dimensional Ising spin glass with Lévy-distributed interactions to test universality. An extended scaling analysis of the correlation length and spin-glass susceptibility suggests that for all values of α the Lévy spin glass obeys universality. Previous claims that universality might be destroyed when $\alpha \rightarrow 1$ possibly stem from the fact that the simulations did not take into account the effects of the strong interactions between some spins, i.e., rendering the simulations nonergodic. Further support for uni-

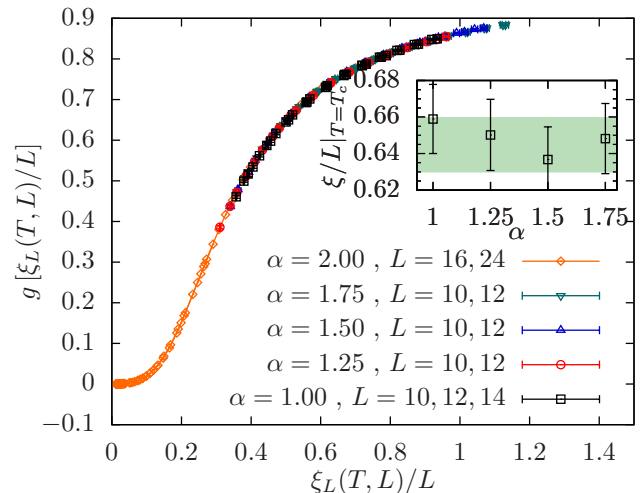


FIG. 5: (Color online) Binder ratio g as a function of the two-point finite-size correlation length ξ_L/L for $\alpha = 1.00, 1.25, 1.50$ and 1.75 for system sizes $L = 10$ and 12 (14 , for $\alpha = 1.00$), as well as 16 and 24 for the Gaussian ($\alpha = 2.0$) case.²⁶ The line is a guide to the eye. All data collapse onto a universal curve, thus providing further evidence for universality. The inset shows $\xi_L/L(T = T_c)$ —also a universal quantity—as a function of α . For all values of α studied the data agree within error bars. The horizontal shaded area corresponds to the best estimate for bimodal disorder $\xi_L/L(T = T_c) = 0.645(15)$.²⁷

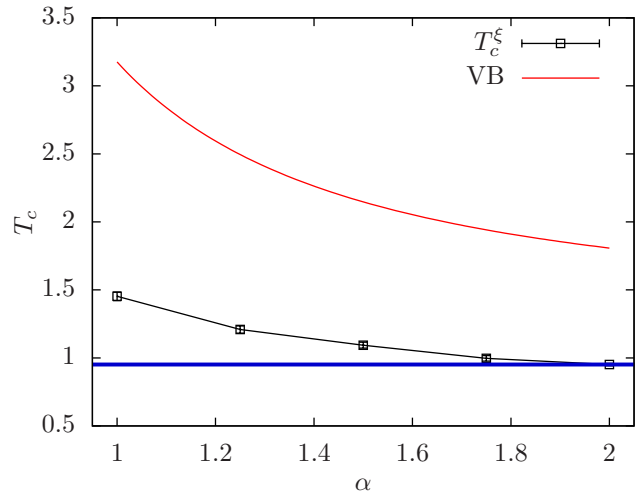


FIG. 6: (Color online) Critical temperature T_c computed from a finite-size scaling of the two-point correlation length, Eq. (7), using the extended scaling technique, Eq. (9). The continuous curve (labeled with VB) is the critical temperature T_c for a mean-field spin glass on a diluted graph with fixed connectivity $k + 1 = 6$. The horizontal thick line represents the critical temperature T_c for the Gaussian spin glass.²⁶

versal behavior is given by the plot of g against ξ_L/L , Fig. 5, where data for all the models studied collapse onto a single universal curve. We do find strong corrections to scaling and therefore studies with larger system sizes and a clear understanding of scaling corrections would

be desirable. However, we find no clear evidence for the lack of universality.

No. PP002-114713). The authors acknowledge ETH Zurich for CPU time on the Brutus cluster.

Acknowledgments

We thank A. K. Hartmann for numerous discussions. H.G.K. acknowledges support from the SNF (Grant

-
- ¹ D. Daboul, I. Chang, and A. Aharony, Euro. Phys. J. B **41**, 231 (2004).
² K. Binder and A. P. Young, Rev. Mod. Phys. **58**, 801 (1986).
³ A. T. Ogielski and I. Morgenstern, Phys. Rev. Lett. **54**, 928 (1985).
⁴ A. T. Ogielski, Phys. Rev. B **32**, 7384 (1985).
⁵ W. L. McMillan, Phys. Rev. B **31**, 340 (1985).
⁶ R. R. P. Singh and S. Chakravarty, Phys. Rev. Lett. **57**, 245 (1986).
⁷ A. J. Bray and M. A. Moore, Phys. Rev. B **31**, 631 (1985).
⁸ R. N. Bhatt and A. P. Young, Phys. Rev. Lett. **54**, 924 (1985).
⁹ R. N. Bhatt and A. P. Young, Phys. Rev. B **37**, 5606 (1988).
¹⁰ N. Kawashima and A. P. Young, Phys. Rev. B **53**, R484 (1996).
¹¹ L. W. Bernardi, S. Prakash, and I. A. Campbell, Phys. Rev. Lett. **77**, 2798 (1996).
¹² D. Iñiguez, G. Parisi, and J. J. Ruiz-Lorenzo, J. Phys. A **29**, 4337 (1996).
¹³ B. A. Berg and W. Janke, Phys. Rev. Lett. **80**, 4771 (1998).
¹⁴ E. Marinari, G. Parisi, and J. J. Ruiz-Lorenzo, Phys. Rev. B **58**, 14852 (1998).
¹⁵ M. Palassini and S. Caracciolo, Phys. Rev. Lett. **82**, 5128 (1999).
¹⁶ P. O. Mari and I. A. Campbell, Phys. Rev. E **59**, 2653 (1999).
¹⁷ H. G. Ballesteros, A. Cruz, L. A. Fernandez, V. Martin-Mayor, J. Pech, J. J. Ruiz-Lorenzo, A. Tarancon, P. Tellez, C. L. Ullod, and C. Ungil, Phys. Rev. B **62**, 14237 (2000).
¹⁸ P. O. Mari and I. A. Campbell (2001), (cond-mat/0111174).
¹⁹ P. O. Mari and I. A. Campbell, Phys. Rev. B **65**, 184409 (2002).
²⁰ T. Nakamura, S.-i. Endoh, and T. Yamamoto, J. Phys. A **36**, 10895 (2003).
²¹ M. Pleimling and I. A. Campbell, Phys. Rev. B **72**, 184429 (2005).
²² T. Jörg, Phys. Rev. B **73**, 224431 (2006).
²³ M. Ostili, J. Stat. Mech. P10005 (2006).
²⁴ I. A. Campbell, K. Hukushima, and H. Takayama, Phys. Rev. Lett. **97**, 117202 (2006).
²⁵ F. P. Toldin, A. Pelissetto, and E. Vicari, J. Stat. Mech. P06002 (2006).
²⁶ H. G. Katzgraber, M. Körner, and A. P. Young, Phys. Rev. B **73**, 224432 (2006).
²⁷ M. Hasenbusch, A. Pelissetto, and E. Vicari, Phys. Rev. B **78**, 214205 (2008).
²⁸ F. Romá, Phys. Rev. B **82**, 212402 (2010).
²⁹ M. Henkel and M. Pleimling, Europhys. Lett. **69**, 524 (2005).
³⁰ K. Janzen, A. K. Hartmann, and A. Engel, J. Stat. Mech. P04006 (2008).
³¹ S. F. Edwards and P. W. Anderson, J. Phys. F: Met. Phys. **5**, 965 (1975).
³² A. K. Hartmann and H. Rieger, *Optimization Algorithms in Physics* (Wiley-VCH, Berlin, 2001).
³³ K. Binder, Phys. Rev. Lett. **47**, 693 (1981).
³⁴ V. Privman and M. E. Fisher, Phys. Rev. B **30**, 322 (1984).
³⁵ K. Hukushima and K. Nemoto, J. Phys. Soc. Jpn. **65**, 1604 (1996).
³⁶ H. G. Katzgraber, M. Palassini, and A. P. Young, Phys. Rev. B **63**, 184422 (2001).
³⁷ R Core Team, URL <http://cran.r-project.org>.
³⁸ I. Neri, F. L. Metz, and D. Bollé, J. Stat. Mech. P01010 (2010).
³⁹ D. J. Thouless, Phys. Rev. Lett. **56**, 1082 (1986).
⁴⁰ P. Cizeau and J. P. Bouchaud, J. Phys. A **26**, L187 (1993).